

Adaptive Control of Holonomic Constrained Systems: A Feedforward Fuzzy Approximation-Based Approach

Chian-Song Chiu, *Member, IEEE*, Kuang-Yow Lian, *Member, IEEE*, and Peter Liu

Abstract—This paper proposes a novel adaptive fuzzy control scheme for the motion/force tracking control of holonomic constrained systems with poorly understood models and disturbances. Some disadvantages of traditional adaptive fuzzy controllers are removed here. In comparison to typical state-feedback fuzzy approximation, the uncertainties are compensated based on a feedforward fuzzy approximation (FFA), which takes desired commands as the premise variables of fuzzy rules. In detail, a unified control model is introduced for representing well-known holonomic systems with an environmental constraint or a set of closed kinematic chains. Then, the FFA-based fuzzy system, adaptation mechanism, and auxiliary-compensating control are derived to ensure robust motion and force tracking in a global manner. Furthermore, a feasible solution for the derived linear matrix inequality guarantees the attenuation of both disturbances and fuzzy parameter errors in an L_2 -gain sense. Finally, two applications are carried out on: 1) a two-link constrained robot and 2) two planar robots transporting a common object. Numerical simulation results show the expected performance.

Index Terms—Adaptive fuzzy control, H^∞ performance, holonomic systems, linear matrix inequality (LMI), motion/force control.

I. INTRODUCTION

HOLONOMIC mechanical systems represent numerous industrial plants—two, for example, are constrained robots and cooperative multirobot systems. Due to various tasks, such as scribing and/or cooperatively manipulating a common object by multiple robots, an environmental constraint [1] and a set of closed kinematic chains [2], [3] (well-known holonomic constraints) are usually imposed on dynamic systems. Arising from the different types of holonomic constraints, the two cases are often considered separately in controller design. From the pioneering work in [1], a reduced-state-based approach is utilized in most researches [2]–[4]. When considering parametric uncertainties, adaptive control schemes were introduced in [5]–[8]. Unfortunately, the reduced-state-based approach usually has a

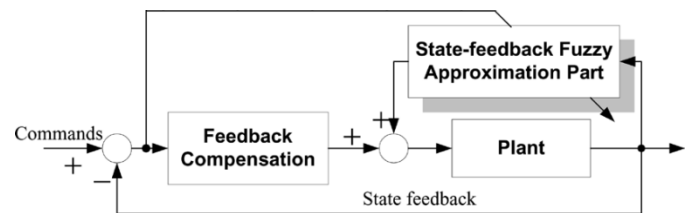


Fig. 1. Configuration of SFA-based adaptive controller.

force-tracking residual error proportional to estimated parameter errors. Thus, a high gain-force feedback or acceleration feedback is needed (e.g., [5] and [7]). An alternative hybrid motion/force control stated in [9] has assured both motion and force tracking errors to be zero. To deal with unstructured uncertainties, several robust control strategies [10]–[12] provide asymptotic motion tracking and an ultimate bounded force error. In contrast to discontinuous control laws, the works in [13] and [14] apply adaptive fuzzy control to compensate unmodeled uncertainties and achieve H^∞ tracking performance. However, their applications are limited due to high computation load arising from the numerous fuzzy rules and tuning parameters.

Plenty of adaptive fuzzy control methods [12]–[21] have been proposed to deal with the control problem of poorly modeled plants. All of this research is based on the universal approximation theorem (first proposed by Wang and Mendel [15]) and the feedback-error-linearizing (FEL) method (first proposed by Miyamoto *et al.* [22]). For these methods, the uncertain dynamics are approximated by a fuzzy system in terms of a linear-in-parameter structure, while the controlling error is used to tune the parameters for stability. The configuration of these controllers is shown in Fig. 1. Since the feedback state is taken as the input of fuzzy approximator, we call these controllers the state-feedback fuzzy approximation (SFA) based controllers. The SFA-based control contains the following disadvantages: 1) numerous fuzzy rules and tuning parameters are required, especially for multivariable systems; 2) the fuzzy approximation error is assumed *a priori* to be upper bounded, although the bound depends on state variables. To remove the above limitations, the author [23] proposes the feedforward fuzzy approximation (FFA) based controller, which takes the forward command as the input of fuzzy approximator as shown in Fig. 2. At first glance, the FFA-based control method also belongs to a class of the FEL-based control methods, since the feedback error is used for tuning parameters of the compensator, but a closer investigation reveals the difference in: 1) the type of training signals and 2) the process of taming dynamic

Manuscript received June 7, 2005; revised October 26, 2005. Manuscript received in final form January 9, 2006. Recommended by Associate Editor Y. Jin. This work was supported by the National Science Council, R.O.C., under Grants NSC-93-2213-E-270-001 and NSC-93-2213-E-033-008.

C.-S. Chiu is with the Department of Electronic Engineering, Chien-Kuo Technology University, Changhua 50050, Taiwan, R.O.C. (e-mail: cschiu@ctu.edu.tw).

K.-Y. Lian is with the Department of Electrical Engineering, Chung-Yuan Christian University, Chung-Li 32023, Taiwan, R.O.C. (e-mail: lian@dec.ee.cycu.edu.tw).

P. Liu is with the BG Networking and Communications, BENQ Corporation, Taipei, Taiwan 114, R.O.C.

Digital Object Identifier 10.1109/TCST.2006.872527

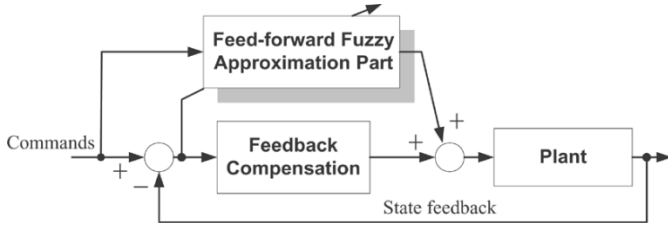


Fig. 2. Configuration of FFA-based adaptive controller.

uncertainties. Although the merits of the FFA over the FEL cannot be quantitatively shown, the FFA-based controller has a simpler architecture of implementation compared to traditional FEL-based controllers (SFA-based controllers). Unfortunately, the FFA-based control still lacks a rigorous stability analysis in current literature. It is also noted that a common situation of all studies cited above is in defect of considering the effect due to the estimated fuzzy parameter errors. All of these points motivate further research on improving the FFA-based control.

To solve the aforementioned problems, this paper proposes an FFA-based adaptive control scheme for motion/force tracking of poorly modeled holonomic systems. To handle the motion/force tracking problem for holonomic systems, we first formulate the typical two cases into a fully actuated system with constraints. Then, the reduced-state-based approach [1] is extended to achieve separate design of motion and force control. Furthermore, the FFA-based adaptive controller is derived to eliminate the effect due to uncertainties and disturbances. Indeed, the main concept of the FFA-based control is taking desired commands as the premise variables of fuzzy rules and approximately compensating an unknown feedforward term required during steady state. Hence, the proposed controller is no longer with the disadvantages of the traditional FEL-based (or SFA-based) adaptive controllers mentioned above. Meanwhile, the stability is guaranteed in a rigorous analysis via Lyapunov's method. In addition, the attenuation of both disturbances and estimated fuzzy parameter errors is achieved in an L_2 -gain sense, while the LMI techniques [24], [25] are used to simplify the gain design. Notice that the proposed approach assures the global stability of both motion and force tracking in a straightforward manner. Compared to the relative works [13] and [14], we deal with more general holonomic systems subject to environmental constraint or closed kinematic chains ([13] and [14] only consider a special case in holonomic systems). Moreover, our proposed scheme achieves both robust motion and force-tracking control (but [13] does not). Meanwhile, the scheme has a novel architecture which can be easily implemented.

The remainder of this paper is organized as follows. The general model of holonomic constrained systems is formulated in Section II, while some useful properties are introduced. In Section III, the FFA-based adaptive controller is developed for holonomic systems. Section IV shows the simulation results of controlling two typical holonomic systems, which are a constrained robot and a cooperative multirobot system transporting a common object. Finally, some concluding remarks are made in Section V.

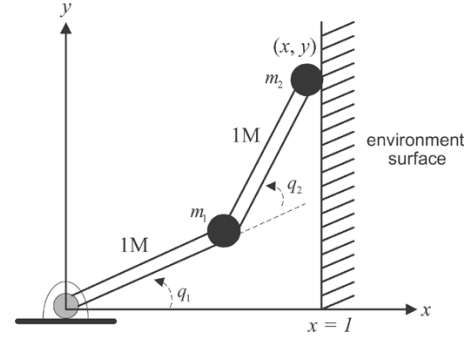


Fig. 3. Two-link planar constrained robot manipulator.

II. MODELING AND PROPERTIES

A. Model Descriptions

Consider a nonredundant holonomic system with a generalized coordinate $q \in R^n$ and the holonomic constraint $\phi(q) = 0$ and $A(q)\dot{q} = 0$, where $\phi : R^n \mapsto R^m$ and $A(q) = \partial\phi(q)/\partial q$. Without loss of generality, we assume that the system is operated away from any singularity with the exactly known function $\phi(q) \in C^2$. From investigation on well-known holonomic systems, different model descriptions exist due to the two kinds of constraints—an environmental constraint and a set of closed kinematic chains. Nevertheless, the model's general form is able to be formulated into a fully actuated system with a constraint.

First, consider an environmental constraint. The motion equation is expressed as (cf. [1])

$$M(q)\ddot{q} + C(q, \dot{q})\dot{q} + g(q) + \tau_d(t) = B(q)\tau + A^\top \lambda \quad (1)$$

where $M(q)$, $C(q, \dot{q})\dot{q}$, and $g(q)$ are the inertia matrix, Coriolis/centrifugal force, and gravitational force, respectively (which are continuous and assumed to be poorly known); $\tau_d(t)$ is a bounded external disturbance; $\tau \in R^n$ is an applied force; $B(q)$ is an invertible input matrix; and $\lambda \in R^m$ is a Lagrange multiplier which physically presents a reaction force from rigid contact. A typical example is the constrained robot manipulator, as illustrated in Fig. 3.

Second, consider the constraint arising from a set of closed kinematic chains. The motion equation can be written as (cf. [2] and [3])

$$M(q)\ddot{q} + C(q, \dot{q})\dot{q} + g(q) + \tau_d(t) = \begin{bmatrix} 0_{(n-m) \times 1} \\ B_2(q)\tau \end{bmatrix} + \begin{bmatrix} A_1^\top \\ A_2^\top \end{bmatrix} \lambda \quad (2)$$

where a proper coordinate manipulation has been utilized; $\tau \in R^m$ is an applied force; $B_2(q)$ is an invertible input matrix; and $A(q)$ is partitioned into $A = [A_1 \ A_2]$ with a full column rank $A_1 \in R^{m \times (n-m)}$ ($(n-m) \leq m$). A good example is the cooperative multirobot system, i.e., multiple robots transporting an object as shown in Fig. 4. Since A_1^\top is a nonsquare and full row-rank matrix, there exists a nontrivial null space $\mathcal{Z} = \{\lambda_I \in R^m | A_1^\top \lambda_I = 0\}$. This means that the Lagrange multiplier can be decomposed as $\lambda = \lambda_I + \lambda_M$, where $\lambda_I \in \mathcal{N}(A_1^\top)$ and $\lambda_M \in \mathcal{R}(A_1) = \mathcal{N}(A_1^\top)^\perp$. When λ lies in the null space \mathcal{Z} , the resulting force $A_1^\top \lambda$ has no contribution to the motion of the corresponding coordinate q ,

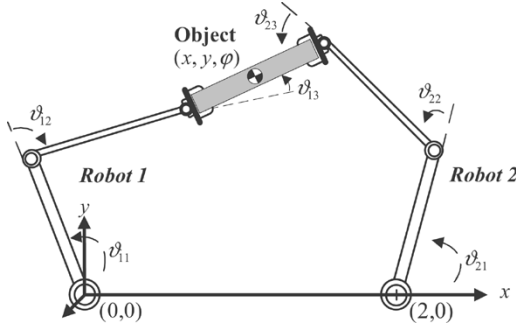


Fig. 4. Two planar cooperative robots transporting a common object.

i.e., only $A_1^\top \lambda_M$ has contribution to the motion. In physical terms, λ_I denotes an internal force while λ_M denotes a motion-inducing force. Therefore, let a virtual control input such as $\tau_v = [(A_1^\top \lambda_M)^\top (\tau + B_2^{-1} A_2^\top \lambda_M)^\top]^\top$ and re-express the right-hand side of (2) in the form $B_v \tau_v + A^\top \lambda_I$ with $B_v = \text{block-diag}\{I_{n-m}, B_2(q)\}$. Referring to (1), the general model of a holonomic system is obtained as

$$M(q)\ddot{q} + C(q, \dot{q})\dot{q} + g(q) + \tau_d(t) = B_g \tau_g + A^\top \lambda_g \quad (3)$$

where the pair (B_g, τ_g, λ_g) is separately denoted accordingly as (B, τ, λ) and (B_v, τ_v, λ_I) for an environmental constraint and a set of closed kinematic chains. After determining the general input τ_g , the actual control input is calculated by

$$\tau = \begin{cases} \tau_g, & \text{for an environmental constraint} \\ \tau_{g2} - B_2^{-1} A_2^\top (A_1^\top)^\dagger \tau_{g1}, & \text{for a set of closed kinematic chains} \end{cases} \quad (4)$$

where $\tau_{g1} \in R^{n-m}$, $\tau_{g2} \in R^m$ are partitioned components of τ_g (i.e., $\tau_g = \tau_v = [\tau_{g1}^\top \ \tau_{g2}^\top]^\top$), and $(A_1^\top)^\dagger = A_1 (A_1^\top A_1)^{-1}$ denotes the pseudo-inverse of A_1^\top . Therefore, the controller design can be performed from a unified viewpoint.

B. Reduced Dynamics and Useful Properties

Since the motion is subject to an m -dimensional constraint, the configuration space of the holonomic system is left with $(n-m)$ degrees of freedom. From the implicit function theorem [1] and an appropriate manipulation of the constraint $\phi(q) = 0$, we find a partition of q as $q = [q_1^\top \ q_2^\top]^\top$ for $q_1 \in R^{n-m}$, $q_2 \in R^m$, such that the generalized coordinate q_2 is expressed in terms of the independent coordinate q_1 as $q_2 = \Omega(q_1)$ with a nonlinear mapping function Ω . Due to the nonsingularity assumption, the terms $\partial\Omega/\partial q_1$ and $\partial^2\Omega/\partial q_1^2$ are bounded in the work space. The generalized displacement and velocity can be expressed in terms of the independent coordinates q_1, \dot{q}_1 as

$$q = [q_1^\top \ (\Omega(q_1))^\top]^\top \quad (5)$$

$$\dot{q} = \begin{bmatrix} I_{n-m} \\ \frac{\partial\Omega(q_1)}{\partial q_1} \end{bmatrix} \dot{q}_1 \equiv J \dot{q}_1. \quad (6)$$

Equations (5) and (6) and the constraint of velocity $A(q)\dot{q} = 0$ lead to $A(q_1)J(q_1)\dot{q}_1 = 0$. Notice that, here, we use $A(q_1)$ to denote $A(q_1, \Omega(q_1))$ for brevity. In other words, $A(q_1)J(q_1) = 0$ since $A(q_1)J(q_1)$ is full column rank and \dot{q}_1 is an independent coordinate (see [1]). Thus, there exists a reduced dynamics for

the holonomic system (3). Due to the velocity transformation (6), the generalized acceleration satisfies $\ddot{q} = J\ddot{q}_1 + \dot{J}\dot{q}_1$. The motion (3) is further represented by the independent coordinates q_1, \dot{q}_1 , and \ddot{q}_1 as

$$M(q_1)J\ddot{q}_1 + \bar{C}(q_1, \dot{q}_1)\dot{q}_1 + g(q_1) + \tau_d(t) = B_g(q_1)\tau_g + A^\top \lambda_g \quad (7)$$

where $\bar{C} = M\dot{J} + CJ$. According to the fact $A(q_1)J(q_1) = 0$, a reduced dynamics [1] is obtained after multiplying J^\top on both sides of (7)

$$\underline{M}(q_1)\ddot{q}_1 + \underline{C}(q_1, \dot{q}_1)\dot{q}_1 + \underline{g}(q_1) + \underline{\tau}_d(q_1, t) = J^\top B_g \tau_g \quad (8)$$

with $\underline{M} = J^\top M J$; $\underline{C} = J^\top \bar{C}$; $\underline{g} = J^\top g$; and $\underline{\tau}_d = J^\top \tau_d$. From the dynamics (8), some useful properties are addressed below.

Property 1: For the partition $I_n = [E_1 \mid E_2]$ with $E_1 = [I_{n-m} \ 0_{(n-m) \times m}]^\top \in R^{n \times (n-m)}$ and $E_2 = [0_{m \times (n-m)} \ I_m]^\top \in R^{n \times m}$, the velocity transformation matrix J satisfies $J^\top E_1 = I_{n-m}$.

Property 2: From the existence of $\Omega(\cdot)$ and the implicit function theorem, A_2 is invertible.

Property 3: The matrix \underline{M} is symmetric and positive-definite while $\underline{M}^{-1} \in L_\infty$.

Property 4: Matrix $(\dot{\underline{M}} - 2\underline{C})$ is skew-symmetric (cf. [1]), i.e., $\zeta^\top (\dot{\underline{M}} - 2\underline{C}) \zeta = 0, \forall \zeta \in R^{n-m}$.

III. FFA-BASED ADAPTIVE CONTROLLER

This section presents an FFA-based adaptive fuzzy controller for controlling holonomic systems. For holonomic systems, the control objective is to track a desired motion trajectory $q_{1d}(t) \in C^2$ while maintaining force λ_g at a desired $\lambda_{gd}(t)$. Due to the constraint motion, the desired motion trajectory should satisfy the kinematic relations (5) and (6). Inspired by pure-motion tracking, some notations are defined as

$$\begin{aligned} e_m &= q_{1d} - q_1, \quad e_m \in R^{n-m} \\ q_a &= \Lambda_m e_m + \dot{q}_{1d}, \quad q_a \in R^{n-m} \\ s &= q_a - \dot{q}_1, \quad s \in R^{n-m} \end{aligned} \quad (9)$$

where e_m, q_a , and s are the motion error, auxiliary signal vector, and error signal, respectively, and $\Lambda_m \in R^{(n-m) \times (n-m)}$ is a symmetric positive-definite matrix. If the system satisfies $\lim_{t \rightarrow \infty} s(t) = 0$, then position and velocity tracking errors e_m and \dot{e}_m exponentially converge to zero. In other words, the error signal s is an error measure deviating from the stable subspace $\{e_m, \dot{e}_m \in R^{n-m} \mid s(t) = 0\}$. The motion tracking problem is, therefore, transformed to the problem of stabilizing $s(t)$. On the other hand, a force-tracking error and force-error filter are accordingly defined as

$$\tilde{\lambda} = \lambda_{gd} - \lambda_g \in R^m \quad (10)$$

$$\dot{e}_\lambda + \eta_1 e_\lambda = \eta_2 \tilde{\lambda}, \text{ with } \eta_1, \eta_2 > 0. \quad (11)$$

Then, the reduced-state-based scheme is to drive the motion trajectory into the stable subspace while the contact force is separately controlled, maintaining a zero e_λ .

In order to derive the adaptive fuzzy controller for uncertain holonomic systems, the error dynamics of s along the motion (7) is written as

$$\begin{aligned} MJ\dot{s} &= MJ\dot{q}_a - MJ\ddot{q}_1 \\ &= -\bar{C}s + f + \tau_d - A^\top \lambda_g - B_g \tau_g \end{aligned} \quad (12)$$

where $f = M(q_1)J(q_1)\dot{q}_a + \bar{C}(q_1, \dot{q}_1)q_a + g(q_1) \in R^n$. Since the term $f(\cdot)$ is assumed to be poorly understood, a direct feedback cancellation is invalid such that a fuzzy approximation-based controller will be utilized to compensate the uncertainties. However, a traditional fuzzy approximation-based controller needs $q_1, \dot{q}_1, q_{1d}, \dot{q}_{1d}$, and \ddot{q}_{1d} as the premise variables for acceptable approximation, since $f(\cdot)$ is a functional of the state variables and reference signals. This will lead to a large computational load on the controller processor. To avoid this situation, an FFA-based control scheme is introduced below.

When the motion tracking goal is achieved, the term $f(\cdot)$ converges to the function $f_d(q_{1d}, \dot{q}_{1d}, \ddot{q}_{1d}) = M(q_{1d})J(q_{1d})\ddot{q}_{1d} + \bar{C}(q_{1d}, \dot{q}_{1d})\dot{q}_{1d} + g(q_{1d})$. Notice that f_d is a feedforward compensation term and is independent to state variables. If the effect of omitting the error $f - f_d$ can be eliminated by feedback of tracking error, the concept of using the forward compensation f_d is feasible. Here, $f_d(\cdot)$ is a much simpler function than $f(\cdot)$, since f_d only depends on the reference signals. According to the above idea, we closely approximate and compensate the forward term $f_d(\cdot)$ by a fuzzy system with the singleton fuzzyfier and product inference. Then, the fuzzy inferred output is

$$\hat{f}_d(z(t), \theta_{f_d}) = Y_{f_d}(z(t))\theta_{f_d} \quad (13)$$

where $z(t)$ is a premise variable vector composed of the reference signals $q_{1d}(t), \dot{q}_{1d}(t)$, and $\ddot{q}_{1d}(t)$; $\theta_{f_d} \in R^{nr \times 1}$ is a fuzzy tuning parametric vector in the consequent part of rules, with r denoting the total number of rules; and $Y_{f_d} = \text{block-diag}\{\xi^\top, \dots, \xi^\top\} \in R^{n \times nr}$ denotes a regression matrix consisting of the fuzzy basis function vector $\xi(z(t)) \equiv [\xi^1 \ \dots \ \xi^r]^\top \in R^r$ with $\xi^l(z(t)) = \mu_l(z(t)) / \sum_{l=1}^r \mu_l(z(t))$, $\mu_l(z(t)) = \prod_{j=1}^p \mathbf{X}_j^l(z_j(t)) \geq 0$ for $l = 1, 2, \dots, r$ and appropriate fuzzy set \mathbf{X}_j^l . Since the fuzzy-inferred output depends only on the reference signals and tuning parameters, we call the fuzzy system a FFA-based fuzzy system.

Usually, we apply a proper projection scheme to keep the tuning parameters within a bounded region to avoid the parametric drift phenomenon. In light of this, an appropriate constraint region of θ_{f_d} is defined by

$$\Omega_{\theta_{f_d}} \equiv \{\theta_{f_d} \in R^{nr} \mid \theta_{f_d}^\top \theta_{f_d} \leq \bar{\theta}_{f_d}, \bar{\theta}_{f_d} > 0\}.$$

Inside the specified set $\Omega_{\theta_{f_d}}$ there exists the so-called optimal approximation parameter which leads to the minimum approximation error for the continuous function f_d (cf. the universal approximation theorem [15]). That is

$$\theta_{f_d}^* \equiv \arg \min_{\theta_{f_d} \in \Omega_{\theta_{f_d}}} \left(\sup_{z \in \bar{U}_z} \|f_d - \hat{f}_d(z(t), \theta_{f_d})\| \right)$$

which provides the most accurate approximation with the minimum error

$$W_{f_d} = f_d - Y_{f_d}(z(t))\theta_{f_d}^*. \quad (14)$$

Note that if the parametric constraint is removed, the optimal approximation parameter $\theta_{f_d}^*$ is still upper bounded (cf. [15]). Since both Y_{f_d} and $\theta_{f_d}^*$ are upper bounded, the optimal inferred output $\hat{f}_d(z(t), \theta_{f_d}^*)$ is always bounded. Meanwhile, the forward term f_d is upper bounded by the magnitude of reference motion trajectories. Therefore, we are able to conclude that the fuzzy approximation error W_{f_d} is upper bounded for $t \geq 0$.

Next, the overall controller is synthesized as follows. Based on the FFA-based fuzzy system (13), the overall control law is set in the form

$$\tau_g = B_g^{-1}[Y_{f_d}\theta_{f_d} + E_1(Ks + \tau_a) - A^\top(\lambda_{gd} + k_f e_\lambda)] \quad (15)$$

where $k_f > 0$ is a force feedback gain; $K \in R^{(n-m) \times (n-m)}$ is a symmetric positive definite matrix; τ_a is an auxiliary input designed later; and the definition of s and e_λ is given in (9) and (11), respectively. Meanwhile, the fuzzy parameter θ_{f_d} is adaptively adjusted by (16), shown at the bottom of the page, with $c(\theta_{f_d}(t_0)) < 0$, where $c(\theta_{f_d}) = (\theta_{f_d}^\top \theta_{f_d} - \bar{\theta}_{f_d} + \varepsilon_f)/\varepsilon_f$ is a projection criterion function with a tunable parameter ε_f satisfying $\bar{\theta}_{f_d} > \varepsilon_f > 0$, and $\gamma > 0$ is an adaptation gain. Note that the above update law is an application of the smooth projection algorithm developed in [26]. The update law assures the following properties: a) $\|\theta_{f_d}(t)\|^2 \leq \bar{\theta}_{f_d}$ for all $t \geq t_0$ and b) $\dot{\theta}_{f_d}^\top \tilde{\theta}_{f_d} + \gamma s^\top J^\top Y_{f_d} \tilde{\theta}_{f_d} \leq 0$ for $\tilde{\theta}_{f_d} \equiv \theta_{f_d}^* - \theta_{f_d}$.

Furthermore, the above controller yields the closed-loop error dynamics described by

$$MJ\dot{s} = -\bar{C}s - E_1(Ks + \tau_a) + Y_{f_d}\tilde{\theta}_{f_d} + \Delta f + w + A^\top(\tilde{\lambda} + k_f e_\lambda) \quad (17)$$

where the control law (15) has been substituted into the dynamic (12); the definition of approximation error W_{f_d} in (14) and $\tilde{\lambda}$ in (10) have been applied; $\Delta f \equiv f - f_d$; and $w \equiv W_{f_d} + \tau_d$. To analyze the convergence of motion and force tracking separately, we further multiply J^\top on both sides of (17) and lead to the motion-tracking error dynamics

$$\underline{M}\dot{s} = -\underline{C}s - Ks + J^\top Y_{f_d}\tilde{\theta}_{f_d} + J^\top \Delta f + \underline{w} + \tau_a \quad (18)$$

$$\dot{\theta}_{f_d} = \begin{cases} \gamma Y_{f_d}^\top Js - c(\theta_{f_d}) \frac{\gamma s^\top J^\top Y_{f_d} \theta_{f_d}}{\theta_{f_d}^\top \theta_{f_d}} \theta_{f_d}, & \text{if } (c(\theta_{f_d}) \geq 0 \text{ and } s^\top J^\top Y_{f_d} \theta_{f_d} > 0) \\ \gamma Y_{f_d}^\top Js, & \text{otherwise} \end{cases} \quad (16)$$

where Property 1 ($J^\top E_1 = I_{n-m}$) and the fact $J^\top(q_1)A^\top(q_1) = 0$ have been applied, and $\underline{w} \equiv J^\top w$. Then, replacing \dot{s} of (17) by (18) and multiplying $A_2^{-\top} E_2^\top$ on both sides of (17), the force-tracking error is obtained as follows:

$$\begin{aligned} \tilde{\lambda} + k_f e_\lambda &= A_2^{-\top} E_2^\top \left(M J M^{-1} (-\underline{C}s - Ks + J^\top Y_{fd} \tilde{\theta}_{fd} \right. \\ &\quad \left. + J^\top \Delta f + \underline{w} + \tau_a) + \overline{C}s - \Delta f - Y_{fd} \tilde{\theta}_{fd} - w \right) \\ &\equiv \varpi(e_m, s, \tilde{\theta}_{fd}, w, t) \end{aligned} \quad (19)$$

where Property 2 ($A_2^{-\top} \in L_\infty$) and the fact $E_2^\top E_1 = 0$ have been applied above. It is a worthwhile note that the perturbed term Δf in (18) arises from the use of the feedforward fuzzy compensation. Nevertheless, the term Δf is upper bounded by motion-tracking errors in the following fashion:

$$\begin{aligned} s^\top J^\top \Delta f &\leq s^\top \left(\Psi_s + \frac{1}{2\kappa^2} I_{n-m} \right) s + \|\Lambda_m e_m\|^2 s^\top \Psi_{se} s \\ &\quad + e_m^\top \left(\Psi_e + \frac{\kappa^2}{2} \Psi_J \right) e_m \end{aligned} \quad (20)$$

where there exist an intermediate parameter $\kappa > 0$ and symmetric positive semidefinite matrices Ψ_s , Ψ_{se} , Ψ_e , and Ψ_J dependent on the desired motion trajectory, control parameter Λ_m , and system parameters. This boundedness is assured for all well-known holonomic mechanical systems (the proof is addressed in the Appendix).

Now, the main results of the FFA-based control approach are stated as follows.

Theorem: Consider the holonomic system (3) using the FFA-based adaptive controller (15) tuned by the update law (16). If the auxiliary input is set as

$$\tau_a = 2P_m e_m + \|\Lambda_m e_m\|^2 \Psi_{se} s + \frac{\rho^2}{4} J^\top Y_{fd} Y_{fd}^\top J s \quad (21)$$

and there exist κ , K , and P_m satisfying the following LMI problem:

$$\begin{aligned} \text{Given } \rho, \Lambda_m > 0 \text{ and } Q = \begin{bmatrix} Q_{11} & Q_{21}^\top \\ Q_{21} & Q_{22} \end{bmatrix} > 0 \\ \text{subject to } \kappa, K, P_m > 0 \\ \begin{bmatrix} K_p - Q_{11} & (*) & (*) \\ K_a \Lambda_m - Q_{21} & K_a - Q_{22} & (*) \\ \kappa \Psi_J^{1/2} & 0 & 2I_{n-m} \end{bmatrix} \geq 0 \end{aligned} \quad (22)$$

with $K_a = K - (\rho^2/4 + 1/2\kappa^2)I_{n-m} - \Psi_s$, $K_p = \Lambda_m^\top K_a \Lambda_m + \Lambda_m^\top P_m + P_m \Lambda_m - \Psi_e$, and $(*)$ represents a symmetric term, then: 1) error signals e_m , \dot{e}_m , e_λ , $\tilde{\lambda}$, and fuzzy parameter θ_{fd} are bounded; 2) error vectors e_m , s , and $\tilde{\lambda}$ have globally uniform ultimate bounds being proportional to the inversion of control gains; 3) the closed-loop system is guaranteed with the robust motion-tracking performance

$$\int_{t_0}^T e_a^\top Q e_a dt \leq V_m(t_0) + \frac{1}{\rho^2} \int_{t_0}^T \left(\|\underline{w}(t)\|^2 + \|\tilde{\theta}_{fd}(t)\|^2 \right) dt \quad (23)$$

for $e_a = [e_m^\top \quad \dot{e}_m^\top]^\top$ and a nonnegative constant $V_m(t_0)$.

Proof: First, we prove the claim a). Consider the Lyapunov function candidate

$$V = \frac{1}{2} s^\top \underline{M} s + e_m^\top P_m e_m + \frac{1}{2\gamma} \tilde{\theta}_{fd}^\top \tilde{\theta}_{fd}$$

with a proper symmetric positive-definite matrix P_m . Along the error dynamics (18) and the fact $\dot{e}_m = -\Lambda_m e_m + s$, the time derivative of V is written as follows:

$$\begin{aligned} \dot{V} &= \frac{1}{2} s^\top (\underline{\dot{M}} - 2\underline{C}) s - s^\top K s - e_m^\top (\Lambda_m^\top P_m + P_m \Lambda_m) e_m \\ &\quad - \|\Lambda_m e_m\|^2 s^\top \Psi_{se} s - \frac{\rho^2}{4} s^\top J^\top Y_{fd} Y_{fd}^\top J s \\ &\quad + s^\top J^\top Y_{fd} \tilde{\theta}_{fd} + \frac{1}{\gamma} \dot{\tilde{\theta}}_{fd}^\top \tilde{\theta}_{fd} + s^\top J^\top \Delta f + s^\top \underline{w} \\ &\leq -s^\top K s - e_m^\top (\Lambda_m^\top P_m + P_m \Lambda_m) e_m \\ &\quad - \|\Lambda_m e_m\|^2 s^\top \Psi_{se} s + s^\top J^\top \Delta f + s^\top \underline{w} \end{aligned}$$

where the definition of τ_a , Property 4, and the update law (16) have been applied, and the above inequality is ensured by the property of the update law (i.e., $s^\top J^\top Y_{fd} \tilde{\theta}_{fd} + (1/\gamma) \dot{\tilde{\theta}}_{fd}^\top \tilde{\theta}_{fd} \leq 0$). Due to the boundedness of Δf as the fashion (20), we further obtain

$$\dot{V} \leq -s^\top K_a s - e_m^\top \Upsilon e_m + \frac{1}{\rho^2} \|\underline{w}\|^2 \quad (24)$$

where $K_a = K - (\rho^2/4 + 1/2\kappa^2)I_{n-m} - \Psi_s$; $\Upsilon = \Lambda_m^\top P_m + P_m \Lambda_m - \Psi_e - (\kappa^2/2)\Psi_J$; and $\rho > 0$. Then, applying the expressions $s = [\Lambda_m \quad I_{n-m}]e_a$ and $e_m = [I_{n-m} \quad 0_{n-m}]e_a$, the inequality (24) is rewritten as

$$\begin{aligned} \dot{V} &\leq -e_a^\top \left(\begin{bmatrix} \Lambda_m^\top K_a \Lambda_m + \Upsilon & \Lambda_m^\top K_a \\ K_a \Lambda_m & K_a \end{bmatrix} - Q \right) e_a \\ &\quad - e_a^\top Q e_a + \frac{1}{\rho^2} \|\underline{w}\|^2. \end{aligned}$$

Thus, if the LMI (22) has a feasible solution, then, for \dot{V} , the following holds:

$$\dot{V} \leq -\alpha_0 \|e_a\|^2 + \frac{1}{\rho^2} \|\underline{w}\|^2 \quad (25)$$

with $\alpha_0 = \lambda_{\min}(Q)$. This means that \dot{V} is negative semidefinite once the system trajectory lies within the region $\{e_a(t) \in R^{2(n-m)} \mid -\alpha_0 \|e_a\|^2 + (1/\rho^2) \|\underline{w}\|^2 \leq 0\}$. Since V is positive-definite and \dot{V} satisfies the inequality (25), we can conclude that $s, e_m, \dot{e}_m \in L_\infty$ and $\tilde{\theta}_{fd}, \theta_{fd} \in L_\infty$. As a result, $\dot{s}, \ddot{e}_m \in L_\infty$ is assured based on the boundedness of all terms on right-hand side of (18). On the other hand, taking the force filter (11) into (19) yields that the force-tracking error is expressed in the form

$$\tilde{\lambda} = \left(1 - \frac{k_f \eta_2}{D + \eta_1 + k_f \eta_2} \right) \varpi(e_m, s, \tilde{\theta}_{fd}, w, t) \quad (26)$$

where D is a differential operator. Since $k_f \eta_2 / (D + \eta_1 + k_f \eta_2)$ is a stable filter and all signals e_m , s , $\tilde{\theta}_{fd}$, and w are bounded, the bounded $\varpi(\cdot)$ implies the boundedness of $\tilde{\lambda}$ and e_λ . Note that, since the boundedness

assumption on the fuzzy approximation error W_{fd} is not utilized here, this proof is achieved in a global sense.

Second, consider the claim b). Since \dot{V} is negative semidefinite outside the compact set $\{\|e_a\| \mid \|e_a\| < (1/\alpha_0\rho) \|\underline{w}\|_\infty\}$ from the inequality (25), the tracking error $e_a(t)$ is globally uniformly ultimately bounded with convergence to a compact residual set. From the fact $V \leq \alpha_1 \|e_a\|^2 + (1/2\gamma)\tilde{\theta}_{fd}^\top \tilde{\theta}_{fd}$ with $\alpha_1 = \sup_t \lambda_{\max}(M_a) > 0$ and

$$M_a = \frac{1}{2}[\Lambda_m I_{n-m}]^\top \underline{M}[\Lambda_m I_{n-m}] + [I_{n-m} 0_{n-m}]^\top P_m [I_{n-m} 0_{n-m}]$$

we rewrite (25) as

$$\dot{V} \leq -\frac{\alpha_0}{\alpha_1} V + \frac{\alpha_0}{\alpha_1} \zeta(t)$$

where $\zeta = (1/2\gamma)\tilde{\theta}_{fd}^\top \tilde{\theta}_{fd} + (\alpha_1/\alpha_0\rho^2) \|\underline{w}\|^2$. Then, the solution of the above inequality leads to that the error trajectory of $e_a(t)$ is shaped by

$$\|e_a(t)\| \leq \sqrt{\frac{1}{\alpha_2} V(t_0) \exp\left(-\frac{\alpha_0}{2\alpha_1}(t-t_0)\right)} + \sqrt{\frac{1}{\alpha_2} \left[1 - \exp\left(-\frac{\alpha_0}{\alpha_1}(t-t_0)\right)\right] \sup_t \zeta(t)}$$

with $\alpha_2 = \inf_t \lambda_{\min}(M_a) > 0$. In other words, the uniform ultimate bound of $e_a(t)$ is

$$\|e_a(t)\| \leq \sqrt{\frac{1}{\alpha_2} \sup_t \zeta(t)} = \bar{\zeta} \left(\frac{1}{\gamma} \tilde{\theta}_{fd}, \frac{1}{\rho} \|\underline{w}\|_\infty \right)$$

which can be adjusted by tuning $\tilde{\theta}_{fd}$ and $1/\rho$. Meanwhile, the residual force-tracking error is

$$\lim_{t \rightarrow \infty} \|\tilde{\lambda}(t)\| \simeq \frac{\eta_1}{\eta_1 + k_f \eta_2} \overline{\varpi}(\bar{\zeta}, \tilde{\theta}_{fd}, \|\underline{w}\|_\infty) \quad (27)$$

with a nonnegative constant $\overline{\varpi} = \sup_t \varpi(t)$ dependent on $\bar{\zeta}$, $\tilde{\theta}_{fd}$, and $\|\underline{w}(t)\|_\infty$.

Third, we prove the claim c). Consider an energy function $V_m = (1/2)s^\top \underline{M}s + e_m^\top P_m e_m$ with a proper symmetric positive-definite matrix P_m . Analogous to the proof of the proposition a), a feasible solution of the LMI (22) leads to

$$\dot{V}_m \leq -e_a^\top Q e_a + s^\top J^\top Y_{fd} \tilde{\theta}_{fd} - \frac{\rho^2}{4} s^\top J^\top Y_{fd} Y_{fd}^\top J s + \frac{1}{\rho^2} \|\underline{w}\|^2.$$

Due to the fact that $s^\top J^\top Y_{fd} \tilde{\theta}_{fd} \leq (\rho^2/4)s^\top J^\top Y_{fd} Y_{fd}^\top J s + (1/\rho^2) \|\tilde{\theta}_{fd}\|^2$, the time derivative of V_m satisfies

$$\dot{V}_m \leq -e_a^\top Q e_a + \frac{1}{\rho^2} \left(\|\underline{w}\|^2 + \|\tilde{\theta}_{fd}\|^2 \right).$$

Therefore, integrating both sides of the above inequality, the robust performance (23) for the motion-tracking objective is as-

TABLE I
COMPARISONS BETWEEN SFA AND FFA BASED SCHEMES

Examples Components	Constrained two-link robot		Cooperative three-link robots	
	SFA	FFA	SFA	FFA
Approximated term	$f(\cdot)$	$f_d(\cdot)$	$f(\cdot)$	$f_d(\cdot)$
Premise Variables	$q_1, \dot{q}_1, q_{1d}, \dot{q}_{1d}, \ddot{q}_{1d}$	$q_{1d}, \dot{q}_{1d}, \ddot{q}_{1d}$	$q_1, \dot{q}_1, q_{1d}, \dot{q}_{1d}, \ddot{q}_{1d}$	$q_{1d}, \dot{q}_{1d}, \ddot{q}_{1d}$
Number of Premise Variables	5	3	15 (5×3)	9 (3×3)
Number of Rules Δ	243 (3 ⁵)	27 (3 ³)	729 (3 ⁵ ×3) _†	81 (3 ³ ×3) _†
Number of fuzzy Parameters	486 (3 ⁵ ×2)	54 (3 ³ ×2)	6561 (729×9)	729 (81×9)
Approximation errors	Assumedly Bounded <i>a priori</i>	Always Bounded	Assumedly Bounded <i>a priori</i>	Always Bounded

Δ : each premise variable has three fuzzy sets. \dagger : using the rule-structure in Fig. 5.

sured. In addition, by integrating both sides of the inequality (25), the robust performance is held as

$$\alpha_0 \int_{t_0}^T \|e_a(t)\|^2 dt \leq V(0) + \frac{1}{\rho^2} \int_{t_0}^T \|\underline{w}(t)\|^2 dt.$$

For zero-state response, we have

$$\|e_a(t)\|_2 \leq \frac{1}{\rho\sqrt{\alpha_0}} \|\underline{w}(t)\|_2$$

which means that the effect from disturbance $\underline{w}(t)$ to tracking error $e_a(t)$ has been attenuated to the prescribed level $1/\rho$. \square

Remark 1: Compared to SFA-based control schemes [13], [14], [18], [19], the proposed approach has better advantages as follows: 1) the FFA-based controller omits some information of feedback such that fewer premise variables and rules are used (i.e., the FFA-based controller has a simpler implementation architecture); 2) since the regression matrix Y_{fd} only depends on the desired motion trajectory, some fuzzy inferred steps can be performed off-line; 3) the control gain design is transformed into solving an LMI problem; and 4) the attenuation of both disturbances and fuzzy parameter errors is achieved such that high robustness to external disturbances and approximation errors is guaranteed regardless of the limitation on initial guesses on tuned parameters. \square

Remark 2: The comparison between SFA- and FFA-based controllers applied to typical holonomic systems is made in Table I. Note here that the SFA-based controller is mainly constructed according to the work [13] such that $q_1, \dot{q}_1, q_{1d}, \dot{q}_{1d}$, and \ddot{q}_{1d} have to be taken as the premise variables. In contrast, the FFA-based controller only needs commands q_{1d}, \dot{q}_{1d} , and \ddot{q}_{1d} as the premise variables. For simplification, the fuzzy rules for controlling cooperative robots are properly reduced by using rule structure in Fig. 5. When each premise variable is associated with three fuzzy sets, the benefits of using the FFA-based controller (fewer rules and tuned parameters) are apparent. Moreover, the fuzzy approximation error of SFA-based controllers needs to be assumedly bounded *a priori*. \square

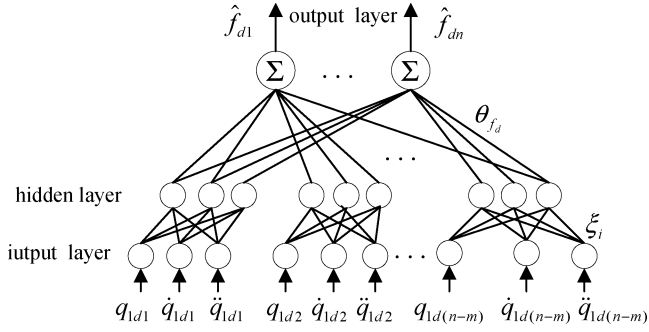


Fig. 5. Rule structure of FFA-based controller for multivariable systems.

IV. SIMULATION RESULTS

To verify the theoretical derivations, we take a constrained robot and a cooperative multirobot system transporting an object as application examples below.

Example 1—Holonomic Constraint as an Environmental Constraint: Consider a two-link planar robot in constrained motion, as shown in Fig. 3, where the end-effector moves along a straight line on a vertical plane. By setting the length of each link as 1 M, the constraint represented in joint space is $\phi(q) = \cos(q_1) + \cos(q_1 + q_2) - 1 = 0$ for $0 \leq q_1 \leq \pi/2$ and $q_1 + q_2 \neq 0$. Then, according to the constraint, the coordinate q_2 is expressed in terms of the independent coordinate q_1 as $q_2 = \arccos(1 - \cos(q_1)) - q_1$. Furthermore, the matrices $A(q)$ and $J(q)$ are accordingly obtained as $A(q) = \begin{bmatrix} -\sin(q_1) - \sin(q_1 + q_2) & -\sin(q_1 + q_2) \end{bmatrix}$ and $J(q) = \begin{bmatrix} 1 & -1 - \sin(q_1)/\sin(q_1 + q_2) \end{bmatrix}^T$ for $q_1 + q_2 \neq 0$. In addition, the dynamics in the general form (3) consists of $B_g = I_2$; $\tau \in R^2$; $\tau_d = [0.25 + 0.25\text{sign}(\sin(\pi t)) \quad 0.25\text{sign}(\sin(\pi t))]^T$

$$M(q) = \begin{bmatrix} \theta_1 + \theta_2 + 2\theta_2 \cos q_2 & \theta_2 + \theta_2 \cos q_2 \\ \theta_2 + \theta_2 \cos q_2 & \theta_2 \end{bmatrix}$$

$$C(q, \dot{q}) = \begin{bmatrix} -\theta_2 \dot{q}_2 \sin q_2 & -\theta_2 (\dot{q}_1 + \dot{q}_2) \sin q_2 \\ \theta_2 \dot{q}_1 \sin q_2 & 0 \end{bmatrix}$$

$$g(q) = \begin{bmatrix} \theta_1 g \cos q_1 + \theta_2 g \cos(q_1 + q_2) \\ \theta_2 g \cos(q_1 + q_2) \end{bmatrix}$$

where $g = 9.81$; $\theta_1 = m_1 + m_2 = 3$; $\theta_2 = m_2 = 1$; and m_1, m_2 are, accordingly, the mass of the first and second links. In this example, the reference commands for motion and force tracking are $q_{1d} = \pi/4 + (\pi/8)\sin(\pi t/2)$ and $\lambda_{gd} = 10 + 2\sin(\pi t/2)$, respectively.

On the other hand, the FFA-based fuzzy system (13) is constructed with q_{1d} , \dot{q}_{1d} , and \ddot{q}_{1d} as premise variables, which are associated with three sets: negative, small, and big. Since the mean and varying region of the premise variables are exactly known (for example, mean of q_{1d} is $\pi/4$ and variance of q_{1d} is $\pi/8$), the membership functions are straightforwardly chosen as

$$\mu_{X_{na}}(q_{1d}) = \frac{1}{(1 + \exp(5(q_{1d} - \frac{\pi}{4} + \frac{\pi}{8})))}$$

$$\mu_{X_{sa}}(q_{1d}) = \exp\left(-2\left(q_{1d} - \frac{\pi}{4}\right)^2\right)$$

$$\mu_{X_{ba}}(q_{1d}) = \frac{1}{(1 + \exp(-5(q_{1d} - \frac{\pi}{4} - \frac{\pi}{8})))}$$

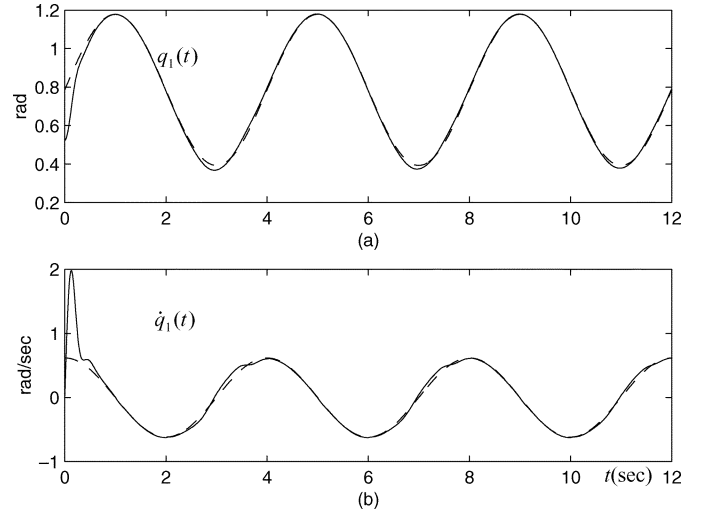


Fig. 6. For the constrained robot: (a) position-tracking result; (b) velocity-tracking result. (— robot, -- reference).

$$\mu_{X_{nb}}(\dot{q}_{1d}) = \frac{1}{(1 + \exp(5(\dot{q}_{1d} + 1)))}$$

$$\mu_{X_{sb}}(\dot{q}_{1d}) = \exp(-\dot{q}_{1d}^2)$$

$$\mu_{X_{bb}}(\dot{q}_{1d}) = \frac{1}{(1 + \exp(-5(\dot{q}_{1d} - 1)))}$$

and

$$\mu_{X_{nc}}(\ddot{q}_{1d}) = \frac{1}{(1 + \exp(5(\ddot{q}_{1d} + 1)))}$$

$$\mu_{X_{sc}}(\ddot{q}_{1d}) = \exp(-\ddot{q}_{1d}^2)$$

$$\mu_{X_{bc}}(\ddot{q}_{1d}) = \frac{1}{(1 + \exp(-5(\ddot{q}_{1d} - 1)))}$$

More partitioned fuzzy sets are available and usually yield a smoother fuzzy inferred output at the price of heavy computation load. Also, although Gaussian membership functions can be shaped by tuning their coefficients, the geometry of membership functions does not obviously affect the control performances. The reason is that the effect of approximation errors can be attenuated in the control. From the fuzzy classification, the total rules of the fuzzy system is 27. The update law (16) is set with $\theta_{fd}(t_0) = 0$, $\gamma = 350$, $\bar{\theta}_{fd} = 10^3$, and $\varepsilon_f = 10$. Here, large values of γ and $\bar{\theta}_{fd}$ are used to obtain better approximation. The reason is that a large γ leads to a large training rate whereas a large $\bar{\theta}_{fd}$ yields a large space of training data. This intuitive observation plays a guideline in choosing the parameters and is confirmed by many simulation results.

Given $\eta_1 = 0.1$, $\eta_2 = 10$, $k_f = 15$, $\Lambda_m = 5$, $\rho = 7$, $Q = 0.5I_2$, and conservatively choosing $\Psi_s = 10$, $\Psi_e = \Psi_{se} = \Psi_J = 1$ due to high uncertainties, the control gains are obtained as $\kappa = 7.4$, $K = 24.2$, and $P_m = 6.3$ from solving the LMI (22). Note that the guidelines of setting parameters are: 1) the residual force error is reduced by a small η_1 and large η_2 , k_f from (27); and 2) larger Λ_m , ρ , Q , Ψ_s , Ψ_e , Ψ_{se} , and Ψ_J lead to smaller motion errors. When the initial states are $q_1(0) = \pi/6$, $q_2(0) = \arccos(1 - \cos(\pi/6)) - \pi/6$, and $\dot{q}(0) = 0$, the proposed controller (15) yields the motion-tracking results shown in Fig. 6. Meanwhile, the force-tracking result and the control inputs are given in Fig. 7. We can find that the tunable fuzzy

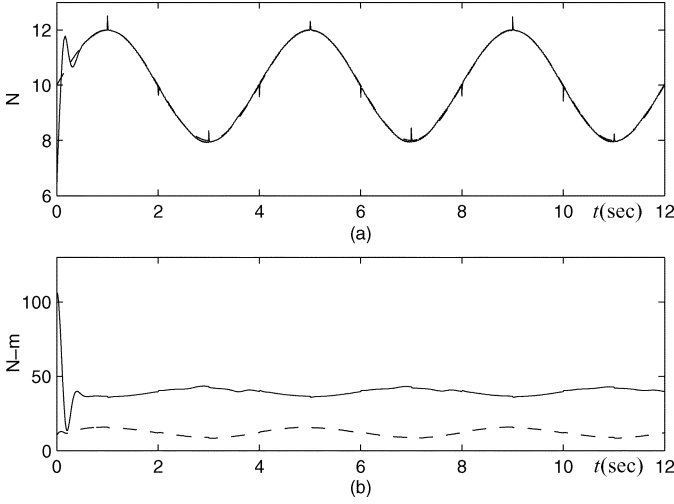


Fig. 7. (a) Response of constraint force (—) and desired force (---). (b) Control inputs for Link-1 (—) and Link 2 (---).

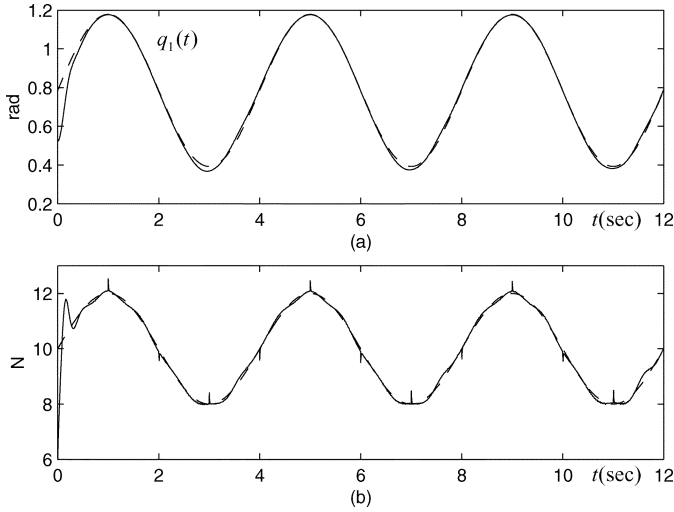


Fig. 8. For an uncertain constraint: (a) position-tracking result; (b) force-tracking result. (— actual, --- reference).

parameters have an upper bound $\theta_{fd}^\top \theta_{fd} \leq 680$ in the steady state, i.e., the simulation confirms the theoretical result. Furthermore, to show the high robustness of our proposed method, we consider a worse environment with an uncertain constraint $\phi(q) = \phi^*(q) + \delta\phi(q, t)$, where $\phi^*(q)$ is a nominal constraint same as the above normal case; and $\delta\phi(q, t) = \pm 0.05 \cos(q_1) - 0.01 \sin(4\pi t)$ is an unknown part of the constraint. When applying the controller based on the above setting for the nominal constraint, the position and force-tracking results are illustrated in Fig. 8. Thus, the satisfactory tracking performance are sustained. \square

Example 2—Holonomic Constraint as a Set of Closed Kinematic Chains: Consider two three-link planar robots cooperatively transporting a common object to be illustrated in Fig. 4. Two robots are identical in mass and length of links. The center of mass for each link is assumed at the end of each link. All the lengths of the first and second links l_1, l_2 , and the held object are 1 M. The length of the third link is sufficiently short and is

taken as a part of the object. Let (x, y, φ) denote the position and orientation of the held object. Let $\vartheta_{1\ell}, \vartheta_{2\ell}$ ($\ell = 1, 2, 3$) denote joint angles of two robots, respectively. The configuration coordinate of the system is, thus, denoted as $q_1 = [x \ y \ \varphi]^\top$ and $q_2 = [\vartheta_{11} \ \vartheta_{12} \ \vartheta_{13} \ \vartheta_{21} \ \vartheta_{22} \ \vartheta_{23}]^\top$. Due to the fact that all the end effectors are rigidly attached to the common object, the holonomic constraint $\phi(q) = [\phi_1^\top(q) \ \phi_2^\top(q)]^\top \in R^6$ consists of

$$\begin{aligned} \phi_1(q) &= \begin{bmatrix} x - 0.5 \cos \varphi \\ y - 0.5 \sin \varphi \\ \varphi \end{bmatrix} - \psi_1 = 0 \\ \phi_2(q) &= \begin{bmatrix} x + 0.5 \cos \varphi - 2 \\ y + 0.5 \sin \varphi \\ \varphi + \pi \end{bmatrix} - \psi_2 = 0 \\ \psi_j &= \begin{bmatrix} \cos(\vartheta_{j1}) + \cos(\vartheta_{j1} + \vartheta_{j2}) \\ \sin(\vartheta_{j1}) + \sin(\vartheta_{j1} + \vartheta_{j2}) \\ \vartheta_{j1} + \vartheta_{j2} + \vartheta_{j3} \end{bmatrix}, \text{ for } j = 1, 2. \end{aligned}$$

Therefore, the Jacobian matrix $A(q)$ is consists of $A_1^\top = \text{block-diag}\{A_{11}^\top, A_{12}^\top\}$ and $A_2 = \text{block-diag}\{A_{21}, A_{22}\}$ with

$$\begin{aligned} A_{11}^\top &= \begin{bmatrix} 1 & 0 & 0 \\ 0 & 1 & 0 \\ 0.5 \sin \varphi & -0.5 \cos \varphi & 1 \end{bmatrix} \\ A_{12}^\top &= \begin{bmatrix} 1 & 0 & 0 \\ 0 & 1 & 0 \\ -0.5 \sin \varphi & 0.5 \cos \varphi & 1 \end{bmatrix} \\ A_{2j} &= - \begin{bmatrix} -\sin(\vartheta_{j1}) - \sin(\vartheta_{j12}) & -\sin(\vartheta_{j12}) & 0 \\ \cos(\vartheta_{j1}) + \cos(\vartheta_{j12}) & \cos(\vartheta_{j12}) & 0 \\ 1 & 1 & 1 \end{bmatrix} \end{aligned}$$

where $\vartheta_{j12} = \vartheta_{j1} + \vartheta_{j2}$. The transformation matrix is written as $J = [I_3 \ -(A_2^{-1}A_1)^\top]^\top$. In addition, the general dynamic model (3) is composed of $B_g = I_9$, $\tau \in R^6$, $M = \text{block-diag}\{M_0, M_1, M_2\}$, $C = \text{block-diag}\{C_0, C_1, C_2\}$, $g = [g_0 \ g_1 \ g_2]^\top$, $M_0 = \text{diag}\{m_o, m_o, I_o\}$, $C_0 = 0$, $g_0 = [0 \ m_o g \ 0]^\top$

$$\begin{aligned} M_j &= \begin{bmatrix} a_{j1} + 2a_{j2} \cos(\vartheta_{j2}) + a_{j3} & (*) & (*) \\ a_{j2} \cos(\vartheta_{j2}) + a_{j3} & a_{j3} & (*) \\ a_{j4} & a_{j4} & a_{j4} \end{bmatrix} \\ C_j &= \begin{bmatrix} -a_{j2} \sin(\vartheta_{j2}) \dot{\vartheta}_{j2} & -a_{j2} \sin(\vartheta_{j2}) \dot{\vartheta}_{j12} & 0 \\ a_{j2} \sin(\vartheta_{j2}) \dot{\vartheta}_{j1} & 0 & 0 \\ 0 & 0 & 0 \end{bmatrix} \\ g_j &= \begin{bmatrix} \frac{(a_{j1} \cos(\vartheta_{j1}) + a_{j2} \cos(\vartheta_{j1} + \vartheta_{j2}))g}{l_1} \\ \frac{a_{j2} \cos(\vartheta_{j1} + \vartheta_{j2})g}{l_1} \\ 0 \end{bmatrix} \end{aligned}$$

for $j = 1, 2$, where $(*)$ represents a symmetric term; $a_{j1} = (m_{j1} + m_{j2} + m_{j3})l_1^2$; $a_{j2} = (m_{j2} + m_{j3})l_1 l_2$; $a_{j3} = (m_{j2} + m_{j3})l_2^2 + I_{j3}$; $a_{j4} = I_{j3}$; and $m_{j1}, m_{j2}, m_{j3}, I_{j3}, m_o, I_o$ are system parameters. We assume that external disturbance is injected to the first joint of two robots as τ_d , which is a square wave with amplitude 0.25 and frequency 0.5 Hz. The actual value of $(m_o, I_o, a_{11}, a_{12}, a_{13}, a_{14}, a_{21}, a_{22}, a_{23}, a_{24})$ is set as (1, 0.25, 5, 3, 3.05, 0.05, 5, 3, 3.05, 0.05). For this cooperative multirobot

system, the control objective is to track desired trajectories for the object and internal force as

$$q_{1d}(t) = \begin{bmatrix} 1 + 0.25 \cos(t) \\ 1 + 0.25 \sin(t) \\ 0.25 \end{bmatrix}$$

$$\lambda_{gd1} = 40 \begin{bmatrix} \cos \varphi \\ \sin \varphi \\ 0 \end{bmatrix}, \lambda_{gd2} = 40 \begin{bmatrix} -\cos \varphi \\ -\sin \varphi \\ 0 \end{bmatrix}$$

where λ_{gd1} and λ_{gd2} represent the compressed force vector.

On the other hand, the FFA-based fuzzy system (13) is constructed with q_{1d} , \dot{q}_{1d} , \ddot{q}_{1d} as premise variables. Since q_{1d} , \dot{q}_{1d} , \ddot{q}_{1d} have exactly known mean and varying region, each premise variable is associated with three fuzzy sets as follows. In detail, the membership functions of q_{1d} is chosen as

$$\text{for } \ell = 1, 2$$

$$\mu_{\mathbf{X}_{n\ell}}(q_{1d\ell}) = \frac{1}{(1 + \exp(5(q_{1d\ell} - 1 + 0.25)))}$$

$$\mu_{\mathbf{X}_{s\ell}}(q_{1d\ell}) = \exp(-2(q_{1d\ell} - 1)^2)$$

$$\mu_{\mathbf{X}_{b\ell}}(q_{1d\ell}) = \frac{1}{(1 + \exp(-5(q_{1d\ell} - 1 - 0.25)))}$$

$$\text{for } \ell = 3$$

$$\mu_{\mathbf{X}_{n3}}(q_{1d3}) = \frac{1}{(1 + \exp(5(q_{1d3} + 0.25 + \frac{\pi}{16})))}$$

$$\mu_{\mathbf{X}_{s3}}(q_{1d3}) = \exp(-2(q_{1d3} + 0.25)^2)$$

$$\mu_{\mathbf{X}_{b3}}(q_{1d3}) = \frac{1}{(1 + \exp(-5(q_{1d3} + 0.25 - \frac{\pi}{16})))}$$

where $q_{1d\ell}$ is the ℓ th element of q_{1d} . The membership functions of linguistic variables $\dot{q}_{1d\ell}$ and $\ddot{q}_{1d\ell}$ denoted as $z_{d\ell}$ are (for $\ell = 1, 2, 3$)

$$\mu_{\mathbf{X}_{nz\ell}}(z_{d\ell}) = \frac{1}{(1 + \exp(5(z_{d\ell} + 1)))}$$

$$\mu_{\mathbf{X}_{sz\ell}}(z_{d\ell}) = \exp(-z_{d\ell}^2)$$

$$\mu_{\mathbf{X}_{bz\ell}}(z_{d\ell}) = \frac{1}{(1 + \exp(-5(z_{d\ell} - 1)))}. \quad (28)$$

To further simplify the rule base and include human knowledge into fuzzy rules, we take the corresponding components of q_{1d} , \dot{q}_{1d} , and \ddot{q}_{1d} as a group due to that they have higher relationship. Thus, the rule-base structure of the fuzzy system has three layers as shown in Fig. 5. Based on the structure of the fuzzy system, the total rule number is 81. Meanwhile, the adaptation mechanism is set with $\theta_{fd}(t_0) = 0$, $\gamma = 50$, $\bar{\theta}_{fd} = 10^4$, and $\varepsilon_f = 10$. Furthermore, the control parameters are chosen as: $\eta_1 = 0.1$, $\eta_2 = 15$, $k_f = 15$, $\Lambda_m = \text{diag}\{10, 5, 5\}$, $\rho = 3$, and $Q = I_6$. Then, after choosing $\Psi_s = \text{diag}\{40, 10, 10\}$, $\Psi_{se} = \Psi_e = 2I_3$, $\Psi_J = I_3$ for (20), the control gains are obtained as $\kappa = 7.9$, $K = \text{diag}\{49.5, 31.2, 31.2\}$, and $P_m = \text{diag}\{36.5, 51.7, 51.7\}$, by solving the LMI (22). In this simulation, the system begins at the position

$$q(0) = [1 \quad \frac{2-\sqrt{3}}{2} \quad 0 \quad \frac{\pi}{2} \quad -\frac{5\pi}{6} \quad \frac{\pi}{3} \quad \frac{\pi}{2} \quad \frac{5\pi}{6} \quad -\frac{\pi}{3}]^T$$

and all have zero initial velocities, i.e., $\dot{q}(0) = 0$. According to the main Theorem, the simulation results of position and velocity tracking for the object are illustrated in Figs. 9 and 10,

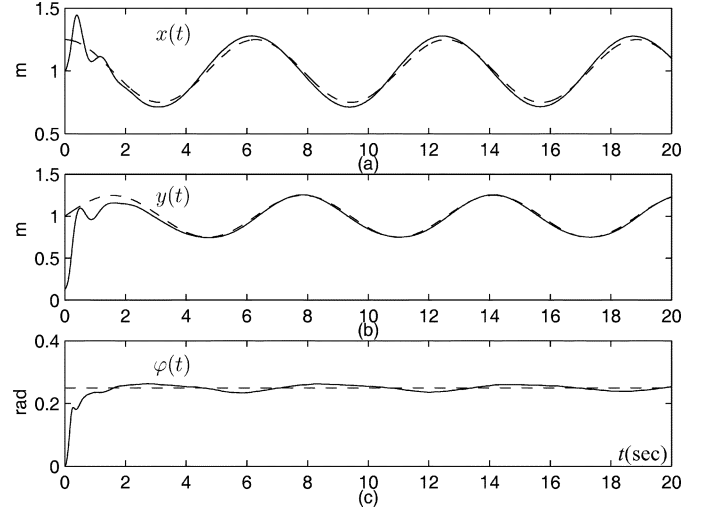


Fig. 9. Position-tracking results of the held object (— object, -- reference).

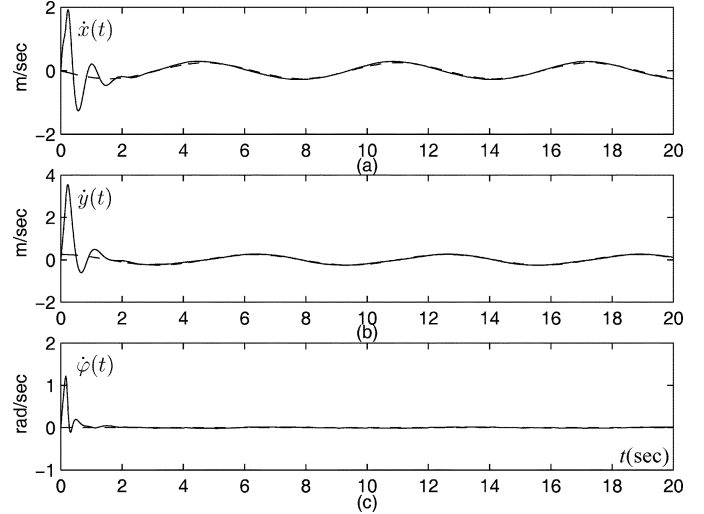


Fig. 10. Velocity-tracking results of the held object (— object, -- reference).

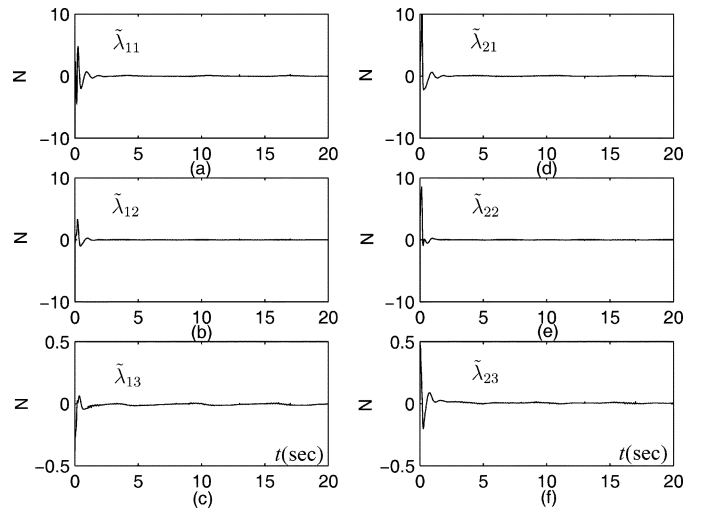


Fig. 11. (a)–(c) Internal force-tracking errors for Robot 1. (d)–(f) Internal force-tracking errors for Robot 2.

respectively. The internal force errors between the desired and actual internal force are shown in Fig. 11. The second joints of two robots are driven by torques illustrated in Fig. 12. The tunable fuzzy parameter is upper bounded by $\theta_{fd}^T \theta_{fd} \leq 7450$ in

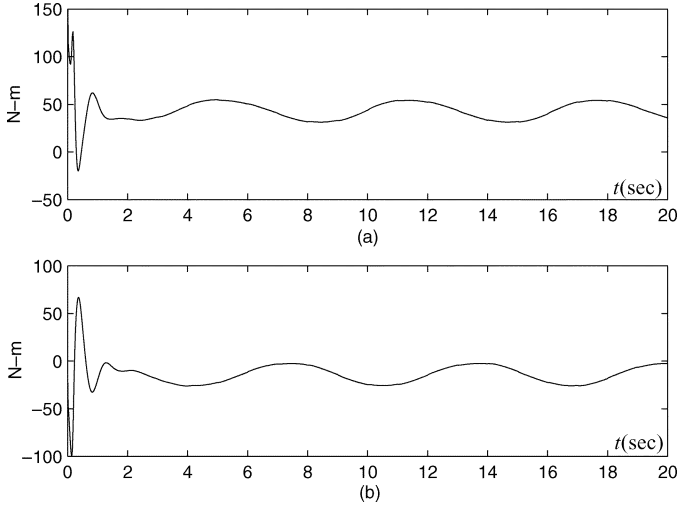


Fig. 12. (a) Control input for the second joint of Robot 1. (b) Control input for the second joint of Robot 2.

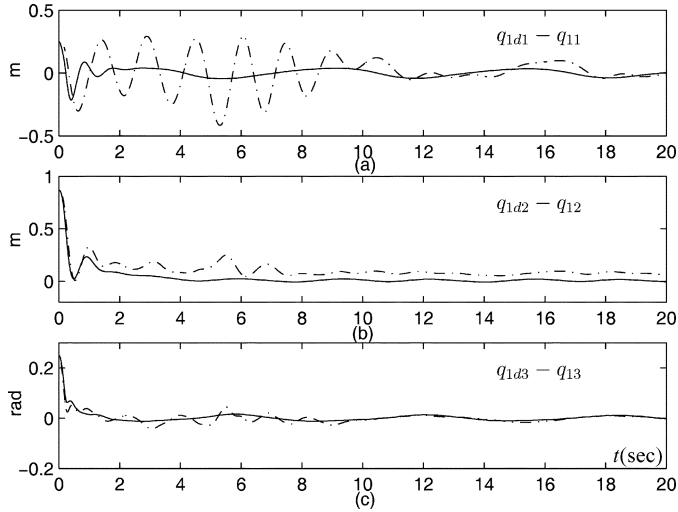


Fig. 13. Comparisons of the position-tracking errors of the held object (— FFA, -- SFA).

the steady state. For a comparison, a traditional SFA-based controller is also constructed and applied to the cooperative robots in which the SFA-based control is set with the same initial conditions and feedback compensation part as the proposed controller, but $\Psi_s = 0$ and $\Psi_e = 0$, $\Psi_{se} = 0$, $\Psi_J = 0$. Then, the position-tracking results for using SFA and FFA-based control are made a comparison given in Fig. 13. Obviously, the FFA-based controller leads to a smaller tracking error. \square

V. CONCLUSION

In this paper, robust motion/force-tracking control of holonomic systems has been solved by the FFA-based adaptive control scheme. Based on the introduced model formulation, typical holonomic systems are represented as a fully actuated system with constraints from a unified viewpoint. The benefit is that the motion/force decomposition control design is performed in a straightforward manner. Furthermore, the FFA-based adaptive control has removed some disadvantages of traditional adaptive fuzzy control including the boundedness assumption on fuzzy

approximation errors, a vast amount of rules and tuning parameters, and complicated implementation architecture. In other words, the proposed scheme is more suitable for complicated or high-dimension systems. By applying an LMI technique, H^∞ motion-tracking performance is guaranteed with the attenuation of disturbances, approximation errors, and tuned fuzzy parameter errors. Meanwhile, the residual force-tracking error is confined to a small value by adjusting control gains feasibly. The simulation results and comparison have shown many benefits which the traditional adaptive fuzzy controllers are lacking.

APPENDIX PROOF OF INEQUALITY (20)

The term $J^\top \Delta f$ can be written in the form

$$J^\top \Delta f = [J^\top(q_1)f - J^\top(q_{1d})f_d] + [(J^\top(q_{1d}) - J^\top(q_1))f_d].$$

According to [27], the first bracket term satisfies

$$\begin{aligned} & s^\top [J^\top(q_1)f - J^\top(q_{1d})f_d] \\ &= s^\top [(\underline{M}(q_1)\dot{q}_r + \underline{C}(q_1, \dot{q}_1)q_r + \underline{G}(q_1)) \\ &\quad - (\underline{M}(q_{1d})\dot{q}_{1d} + \underline{C}(q_{1d}, \dot{q}_{1d})\dot{q}_{1d} + \underline{G}(q_{1d}))] \\ &\leq s^\top \Psi_s s + \|\Lambda_m e\|^2 s^\top \Psi_{se} s + e^\top \Psi_e e \end{aligned}$$

for some symmetric positive semidefinite Ψ_s , Ψ_{se} , and Ψ_e . On the other hand, the second bracket term is represented by

$$\begin{aligned} & (J^\top(q_{1d}) - J^\top(q_1))f_d \\ &= \left[\int_0^1 \frac{\partial J^\top f_d}{\partial q_{11}} (q_{1d} - \varepsilon e) d\varepsilon \cdots \int_0^1 \frac{\partial J^\top f_d}{\partial q_{1(n-m)}} (q_{1d} - \varepsilon e) d\varepsilon \right] e \\ &\equiv H e. \end{aligned}$$

once the mean value theorem is applied. This implies that $s^\top (J^\top(q_{1d}) - J^\top(q_1))f_d \leq (1/2\kappa^2)s^\top s + (\kappa^2/2)e^\top \Psi_J e$, where there exist $\kappa > 0$ and positive semidefinite Ψ_J such that $e^\top H^\top H e \leq e^\top \Psi_J e$. Hence, the inequality (20) is obtained by summarizing the above results. \square

REFERENCES

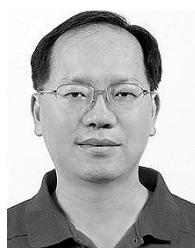
- [1] N. H. McClamroch and D. Wang, "Feedback stabilization and tracking of constrained robots," *IEEE Trans. Autom. Contr.*, vol. 33, no. 5, pp. 419–426, May 1988.
- [2] T. J. Tarn, A. K. Bejczy, and X. Yun, "Design of dynamic control of two cooperating robot arms: Closed chain formulation," in *Proc. IEEE Conf. Robotics and Automation*, 1987, pp. 7–13.
- [3] Z. Li, P. Hsu, and S. Sastry, "Grasping and coordinated manipulation by a multifingered robot hand," *Int. J. Robot. Res.*, vol. 8, pp. 33–50, 1989.
- [4] J. Wang, S. J. Dodds, and W. N. Bailey, "Coordinated control of multiple robotic manipulators handling a common object – Theory and experiments," *Proc. IEE Contr. Theory Appl.*, vol. 144, pp. 103–109, 1997.
- [5] J.-H. Jean and L.-C. Fu, "An adaptive control scheme for coordinated manipulator systems," *IEEE Trans. Robot. Autom.*, vol. 9, no. 2, pp. 226–231, Feb. 1993.
- [6] Y.-H. Liu, S. Arimoto, V. Parra-Vega, and K. Kitagaki, "Decentralized adaptive control of multiple manipulators in cooperations," *Int. J. Contr.*, vol. 67, pp. 649–673, 1997.
- [7] H. Yu and S. Lloyd, "Combined direct and indirect adaptive control of constrained robots," *Int. J. Contr.*, vol. 68, pp. 955–970, 1997.
- [8] W.-H. Zhu and J. D. Schutter, "Control of two industrial manipulators rigidly holding an egg," *IEEE Contr. Syst. Mag.*, vol. 19, no. 2, pp. 24–30, Apr. 1999.
- [9] J. Yuan, "Adaptive control of a constrained robot—Ensuring zero tracking and zero force errors," *IEEE Trans. Autom. Contr.*, vol. 42, no. 12, pp. 1709–1714, Dec. 1997.

- [10] C.-S. Chiu, K.-Y. Lian, and T.-C. Wu, "Robust adaptive motion/force tracking control design for uncertain constrained manipulators," *Automatica*, vol. 40, pp. 2111–2119, 2004.
- [11] R. Y. Zhen and A. A. Goldenberg, "Variable structure hybrid control of manipulators in unconstrained and constrained motion," *ASME J. Dyn. Syst., Meas. Contr.*, vol. 118, pp. 327–332, 1996.
- [12] W. Gueaieb, F. Karray, and S. Al-Sharhan, "A robust adaptive fuzzy position/force control scheme for cooperative manipulators," *IEEE Trans. Contr. Syst. Technol.*, vol. 11, no. 4, pp. 516–528, Jul. 2003.
- [13] Y.-C. Chang and B.-S. Chen, "Robust tracking designs for both holonomic and nonholonomic constrained mechanical systems: Adaptive fuzzy approach," *IEEE Trans. Fuzzy Syst.*, vol. 8, no. 2, pp. 46–66, Feb. 2000.
- [14] K.-Y. Lian, C.-S. Chiu, and P. Liu, "Semi-decentralized adaptive fuzzy control for cooperative multirobot systems with H^∞ motion/internal force tracking performance," *IEEE Trans. Syst., Man, Cybern. B, Cybern.*, vol. 32, no. 3, pp. 269–280, Jun. 2002.
- [15] L. X. Wang and J. M. Mendel, "Fuzzy basis functions, universal approximation, and orthogonal least squares learning," *IEEE Trans. Neural Netw.*, vol. 3, no. 5, pp. 807–814, Sep. 1992.
- [16] B.-S. Chen, C.-H. Lee, and Y.-C. Chang, " H^∞ tracking design of uncertain nonlinear SISO systems: Adaptive fuzzy approach," *IEEE Trans. Fuzzy Syst.*, vol. 4, no. 1, pp. 32–43, Feb. 1996.
- [17] N. Golea and A. Golea, "Fuzzy adaptive control of multivariable nonlinear systems," in *Proc. IEEE FUZZ*, 2002, pp. 330–334.
- [18] H. Lee and M. Tomizuka, "Robust adaptive control using a universal approximator for SISO nonlinear systems," *IEEE Trans. Fuzzy Syst.*, vol. 8, no. 1, pp. 95–106, Feb. 2000.
- [19] W.-S. Lin and C.-S. Chen, "Robust adaptive sliding mode control using fuzzy modeling for a class of uncertain MIMO nonlinear systems," *Proc. Inst. Elect. Eng. Contr. Theory Appl.*, vol. 149, no. 3, pp. 193–201, 2002.
- [20] H. Han, C.-Y. Su, and Y. Stepanenko, "Adaptive control of a class of nonlinear systems with nonlinear parameterized fuzzy approximators," *IEEE Trans. Fuzzy Syst.*, vol. 9, no. 2, pp. 315–323, Apr. 2001.
- [21] M. Alata, C.-Y. Su, and K. Demirli, "Adaptive control of a class of nonlinear systems with a first-order parameterized Sugeno fuzzy approximator," *IEEE Trans. Syst., Man, Cybern. C, Appl. Rev.*, vol. 31, no. 3, pp. 410–419, Aug. 2001.
- [22] H. Miyamoto, M. Kawato, T. Setoyama, and R. Suzuki, "Feedback-error-learning neural networks for trajectory control of a robotic manipulator," *Neural Netw.*, vol. 1, pp. 251–265, 1988.
- [23] Y. Jin, "Decentralized adaptive fuzzy control of robot manipulators," *IEEE Trans. Syst., Man, Cybern. B, Cybern.*, vol. 28, no. 1, pp. 47–57, Feb. 1998.
- [24] S. Boyd, L. E. Ghaoui, E. Feron, and V. Balakrishnan, *Linear Matrix Inequalities in System and Control Theory*. Philadelphia, PA: SIAM, 1994.
- [25] K.-Y. Lian, C.-S. Chiu, T.-S. Chiang, and P. Liu, "LMI-based fuzzy chaotic synchronization and communication," *IEEE Trans. Fuzzy Syst.*, vol. 9, no. 4, pp. 539–553, Aug. 2001.
- [26] J.-B. Pomet and L. Praly, "Adaptive nonlinear regulation: Estimation from the Lyapunov equation," *IEEE Trans. Autom. Contr.*, vol. 37, no. 6, pp. 729–740, Jun. 1992.
- [27] N. Sadeh and R. Horowitz, "Stability and robustness analysis of a class of adaptive controller for robotic manipulators," *Int. J. Robot. Res.*, vol. 9, pp. 74–92, 1990.



Chian-Song Chiu (M'04) received the B.S. degree in electrical engineering and the Ph.D. degree in electronic engineering from the Chung-Yuan Christian University, Chung-Li, Taiwan, R.O.C., in 1997 and 2001, respectively.

He has been an Assistant Professor with Chien-Kuo Technology University, Changhua, Taiwan, since 2003. His current research interests are in robotics, fuzzy systems, and nonlinear control.

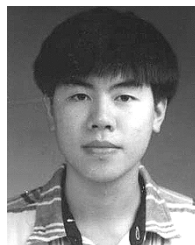


Kuang-Yow Lian (S'91–M'94) received the B.S. degree in engineering science from the National Cheng-Kung University, Tainan, Taiwan, R.O.C., in 1984, and the Ph.D. degree in electrical engineering from National Taiwan University, Taipei, in 1993.

From 1986 to 1988, he was a Control Engineer with ITRI, Hsinchu, Taiwan. He joined Chung-Yuan Christian University, Chung-Li, Taiwan, in 1994, where he is currently a Professor and Chair for the Department of Electrical Engineering. His research interests include nonlinear control systems, fuzzy

control, robotics, chaotic systems, and control system application.

Dr. Lian received the Outstanding Research Award from of the Chung-Yuan Christian University.



Peter Liu received the B.S. and Ph.D. degrees in electrical engineering from Chung-Yuan Christian University, Chung-Li, Taiwan, R.O.C., in 1998 and 2002, respectively.

He is currently an Embedded System Designer with applications in wireless communications with BenQ Corporation, Taipei, Taiwan. His research interests include chaotic systems, nonlinear control, and fuzzy systems.